MICROCOPY RESOLUTION TEST CHART

NATIONAL BUREAU OF STANDARDS-1963-A

AD-A170 847

Investigation of the VUV Radiation Produced by a Sliding Discharge

R. W. F. GROSS, L. E. SCHNEIDER, and S. T. AMIMOTO
Aerophysics Laboratory
Laboratory Operations
The Aerospace Corporation
El Segundo, CA 90245

30 June 1986

Prepared for

SPACE DIVISION
AIR FORCE SYSTEMS COMMAND
Los Angeles Air Force Station
P.O. Box 92960, Worldway Postal Center
Los Angeles, CA 90009-2960

DTIC
SELECTED
AUG 0 5 1986
D

DTIC FILE COPY

86   3   4   037

This report was submitted by The Aerospace Corporation, El Segundo, CA 90245, under Contract No. F04701-85-C-0086 with the Space Division, P.O. Box 92960, Worldway Postal Center, Los Angeles, CA 90009-2960. It was reviewed and approved for The Aerospace Corporation by W. P. Thompson, Jr., Director, Aerophysics Laboratory. Lieutenant Scott W. Levinson, Space Division/YNS, was the project officer for the Mission-Oriented Investigation and Experimentation (MOIE) Program.

This report has been reviewed by the Public Affairs Office (PAS) and is releasable to the National Technical Information Service (NTIS). At NTIS, it will be available to the general public, including foreign nationals.

This technical report has been reviewed and is approved for publication. Publication of this report does not constitute Air Force approval of the report's findings or conclusions. It is published only for the exchange and stimulation of ideas.

SCOTT W. LEVINSON, Lt, USAF
MOIE Project Officer
SD/YNS
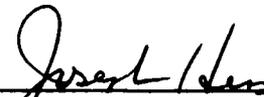
JOSEPH HESS, GM-15
Director, AFSTC West Coast Office
AFSTC/WCO OL-AB

REPORT DOCUMENTATION PAGE	READ INSTRUCTIONS BEFORE COMPLETING FORM

1. REPORT NUMBER	2. GOVT ACCESSION NO.	3. RECIPIENT'S CATALOG NUMBER
SD-TR-86-39	AD-A170847	

4. TITLE (and Subtitle)	5. TYPE OF REPORT & PERIOD COVERED
INVESTIGATION OF THE VUV RADIATION PRODUCED BY A SLIDING DISCHARGE	
	6. PERFORMING ORG. REPORT NUMBER
	TR-0086(6930-01)-7

7. AUTHOR(s)	8. CONTRACT OR GRANT NUMBER(s)
Rolf W. F. Gross, Leo E. Schneider, and Sherwin T. Amimoto	F04701-85-C-0086

9. PERFORMING ORGANIZATION NAME AND ADDRESS	10. PROGRAM ELEMENT, PROJECT, TASK AREA & WORK UNIT NUMBERS
The Aerospace Corporation El Segundo, Calif. 90245	

11. CONTROLLING OFFICE NAME AND ADDRESS	12. REPORT DATE
Space Division Los Angeles Air Force Station Los Angeles, Calif. 90009-2960	30 June 1986
	13. NUMBER OF PAGES
	24

14. MONITORING AGENCY NAME & ADDRESS(if different from Controlling Office)	15. SECURITY CLASS. (of this report)
	Unclassified
	15a. DECLASSIFICATION/DOWNGRADING SCHEDULE

16. DISTRIBUTION STATEMENT (of this Report)

Approved for public release; distribution unlimited.

17. DISTRIBUTION STATEMENT (of the abstract entered in Block 20, if different from Report)

18. SUPPLEMENTARY NOTES

19. KEY WORDS (Continue on reverse side if necessary and identify by block number)

Plasma light source
Sliding discharge
VUV light source

20. ABSTRACT (Continue on reverse side if necessary and identify by block number)

We investigated the electrical characteristics and the vacuum ultraviolet (VUV) radiation produced by a sliding discharge in an atmosphere of argon. The discharge covered the surface of an aluminum rod wrapped with a graded layer of Kapton film from 0.05 to 1.02 mm thick. Rods with diameters of 0.61 cm and 1.23 cm were used. The discharge took place between two electrodes concentric with the aluminum rod, which acted as the return

19. KEY WORDS (Continued)

20. ABSTRACT (Continued)

conductor. A circuit with a ringing frequency of 2.8 μsec half-period and an energy storage capacitor of 1.85 μF charged to 50 kV (2.32 kJ) was used to drive the discharge. Using the smaller rod we observed light pulses of 1.3-μsec FWHM duration which radiated a non-Planckian continuum. About 77 J of the energy emitted by the plasma appeared in the VUV between 140 and 210 nm; this energy corresponds to 3.3% of the energy stored in the capacitor. A peak radiance of 2.8 kW/cm^2 nm was measured at 180 nm; this radiance corresponds to a maximum brightness temperature of 17800 K. In the visible spectrum the radiance was less than 0.06 kW/cm^2 nm, which indicates a much lower brightness temperature of only 12300 K. These characteristics make this discharge an excellent VUV source for a variety of photolytic applications.

CONTENTS

Accesion For		
NTIS CRA&I	☑	
DTIC TAB	☐	
Unannounced	☐	
Justification		
By		
Distribution /		
Availability Codes		
Dist	Avail and/or Special	
A-1		

QUALITY INSPECTED 4

FIGURES

TABLES

I. INTRODUCTION

A sliding discharge is, as its name implies, a large-area, high-current arc between electrodes which "slides" along the surface of a thin insulator covering a metallic return conductor. Figure 1 shows our experimental arrangement. Because the return conductor is very close to the discharge channel, sliding discharges have an inherently low inductance, which makes very fast light sources possible.

Sliding discharges have been used extensively for the preionization of electric discharge lasers[1] and as light sources for the flash-photolytic pumping and initiation of lasers.[2] Since the radiation produced by the plasma of a sliding discharge is not filtered by a quartz envelope, sliding discharges are excellent sources of high-power vacuum ultraviolet (VUV) radiation; in addition, the absence of a quartz envelope removes the limit to the electrical energy dissipation, a limit inherent in ordinary flashlamps.

In this report we describe experiments that study the electrical and radiation characteristics of a coaxial sliding discharge used for photodissociation purposes. To be efficient, such a source should produce radiation only in the wavelength region of interest. This can be accomplished with an optically thin plasma that radiates a nonequilibrium (i.e., a non-Planckian bremsstrahlung continuum originating from free-free and free-bound transitions) in the desired wavelength region. Plasma sources of this kind have been reported by various researchers.[3]

3
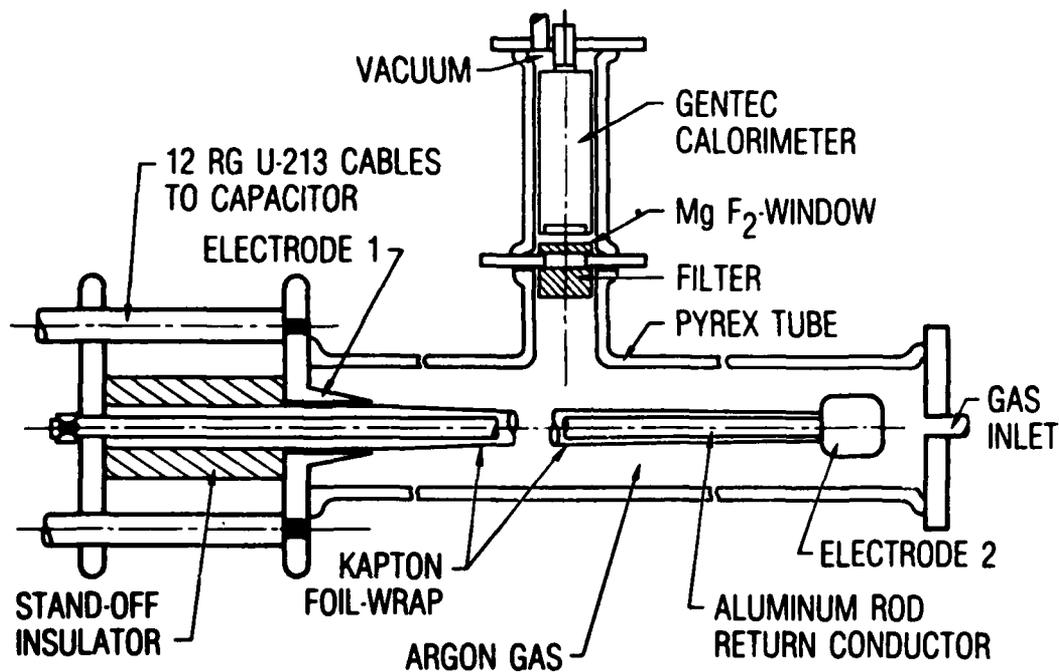
Fig. 1. Experimental Apparatus for the Coaxial Sliding Discharge

II. EXPERIMENTAL APPARATUS

Figure 1 shows a schematic of the sliding discharge we investigated. The discharge took place between two brass electrodes – one surrounding, the other attached to, an aluminum rod serving as a return conductor. The rod was spirally wrapped with a single strip of Kapton film that was 8 cm wide and 0.051 mm (0.002 in.) thick. Because of the overlap of successive layers of the Kapton wrapping, the pitch of the spiral gets smaller and the thickness of the multilayer insulation larger as the winding proceeds along the rod. By trial and error an initial pitch can be found that leads to a parallel winding at the place along the rod where the high-voltage electrode will be located. In this way a graduated winding 0.05 mm thick at one end and 1.02 mm thick at the other was produced, providing the thinnest possible insulating layer that will survive the dielectric stress of the discharge.

We used two different rods: one 6.1 mm in diameter (1/4-in. rod) and with an electrode spacing of 75 cm, the other 12.3 mm in diameter (1/2-in. rod) and with an electrode spacing of 84 cm. Both were wrapped with identical layers of Kapton insulation. The rods were mounted in the center of a Pyrex pipe, 150 cm long and 10 cm in diameter, that could be evacuated by a mechanical vacuum pump and filled with various gases.

Electrical energy was fed to the discharge from a 1.85-μF, 60-kV capacitor (manufactured by Maxwell, Inc.) through 12 parallel RG-U 213 coaxial cables that were each 200 cm long. The multiple, parallel cables provided a capacitor of low inductance that produced an initial high-voltage peak that assured a fast and uniform breakdown of the discharge gap.[4] A specially designed cable ad connected the cables to the rod and the high-voltage electrode. An SF_6-filled spark gap mounted on top of the capacitor triggered the discharge. The spark gap and the ends of the 12 cables at the capacitor side were submerged in transformer oil for insulation. The discharge current was monitored by a Rogowski coil on the shield wire of one of the cables.

The radiation produced by the discharge was observed through a 2.5-cm-diam, UV-grade, MgF_2 window in the Pyrex tube; this window allowed

5

measurements in the spectral region between 120 and 5000 nm. Additional windows of various materials were used as long-wave passband absorption filters to spectrally resolve the radiation emitted into the various wavelength regions. The transmission of these filters was determined by a Beckmann spectrophotometer. We measured the emitted energies with a calibrated optical calorimeter (manufactured by Gentec, Inc.) that was housed in an evacuated side arm of the Pyrex tube.

A photomultiplier equipped with a stack of Corning absorption filters recorded the temporal variation of the light output from the discharge in the near UV between 350 and 450 nm. We tacitly assumed that the time dependence of the VUV light output followed that in the near UV. An electronic streak camera (Hadland, Ltd.) with a streak speed of 1 mm/μsec was used to observe optically the expansion of the luminous plasma surrounding the rod. This camera had an S1 cathode and looked through the Pyrex vacuum envelope; it therefore recorded only radiation emitted into the visible region at wavelengths above 350 nm.

III. EXPERIMENTAL RESULTS

Figure 2 shows an oscilloscope record of the discharge current in the circuit when the discharge gap had been shortened by a wire braid coaxially surrounding the rod. The short-circuit half-period of the freely ringing discharge was found to be 2.8 μsec, which corresponds to a full width at half maximum (FWHM) duration of 1.5 μsec. With a capacitor of 1.85 μF, this indicates a circuit inductance of 225 nH.

Figure 3 shows an oscilloscope trace of the current measured with the sliding discharge actually taking place in an atmosphere of 300 Torr of argon. Argon was chosen because it promised a strong bound-free continuum in the VUV wavelength region; argon has also been shown to have one of the lowest breakdown thresholds for sliding discharges.[5]

It can be seen that the circuit is critically damped by the discharge. Critical damping is desirable, not only because it insures the capacitor a long lifetime, but also because with critical damping a maximum of energy is delivered to the discharge in the shortest time. We found that the damping of the electric discharge is a strong function of gas pressure. For a charging voltage of 50 kV, critical damping occurred at 300 Torr of argon. However, critical damping did not depend strongly on the charging voltage of the capacitor. At 50 kV and 300 Torr argon we measured a peak current of 22 kA in the discharge. The energy stored in the capacitor was 2.31 kJ.

The most interesting observation in Fig. 3 is, however, that the current pulse has a duration almost twice as long as the FWHM of the half-period of the shortened circuit shown in Fig. 2. At 50 kV and 300 Torr argon, we measured a FWHM current pulse duration of 2.8 μsec for the active discharge. This indicates that additional damping mechanisms introduced by the sliding discharge lengthen the current's pulse duration.

To determine the dimensions of the radiating plasma and at the same time study its dynamics, we observed the sliding discharge with the fast-streak camera at a place about halfway between the electrodes. Figure 4 shows a
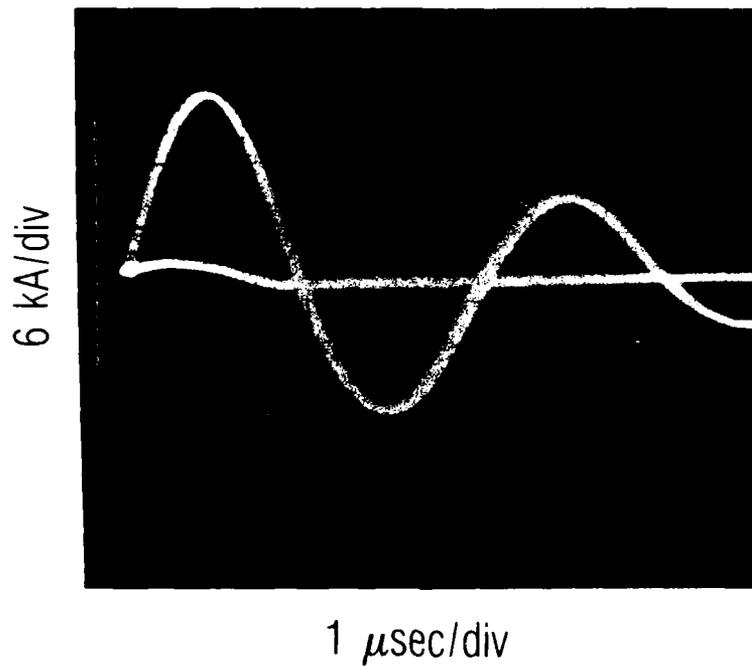
Fig. 2.   Oscilloscope Record of Sliding Discharge Current for a
Shortened Discharge Gap (1/4-in. Rod)

8

6 kA/div

1 μsec/div
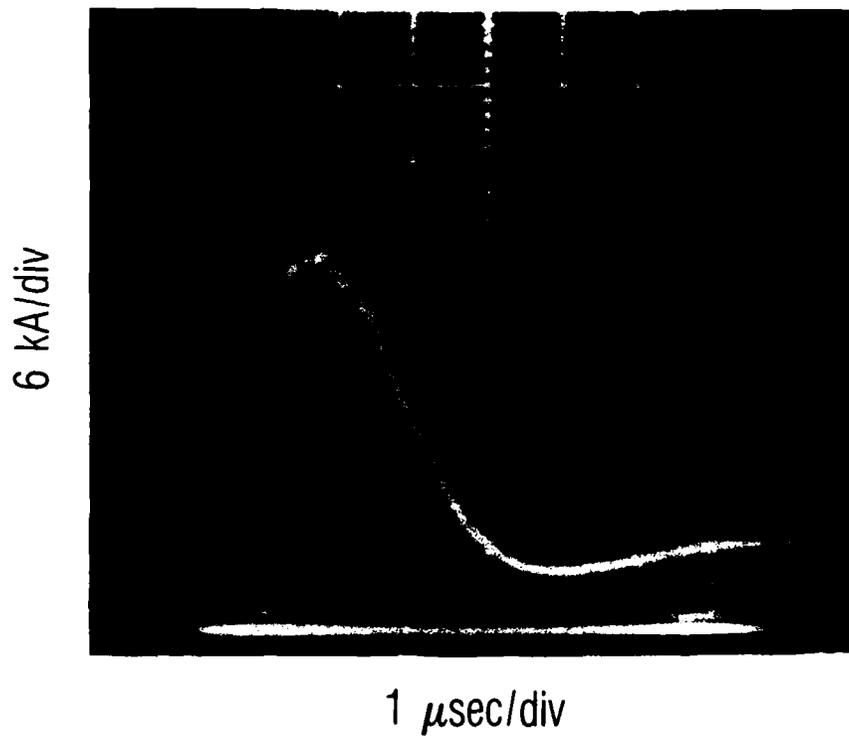
Fig. 3. Oscilloscope Record of Sliding Discharge Current in 300 Torr Argon at 50 kV (1/4-in. Rod)

9
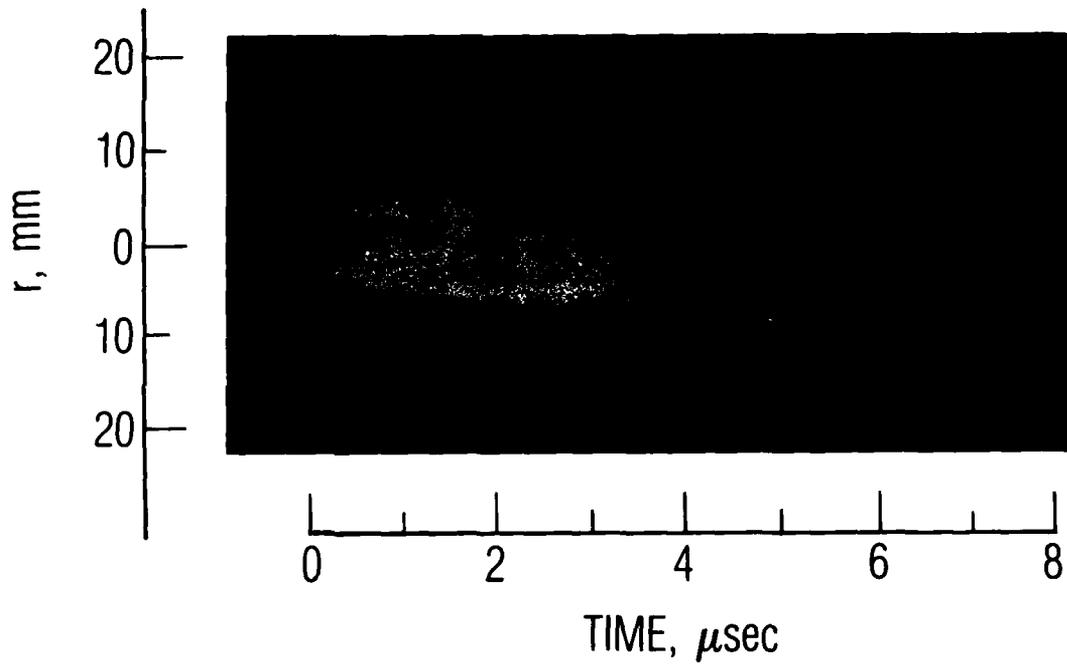
Fig. 4. Streak Camera Record of Discharge Plasma in 300 Torr Argon at 50 kV (1/4-in. Rod)

typical streak photograph. The streak slit of 20-μm width was arranged so it
was perpendicular to the long axis of the rod. Time increases from left to
right as indicated. The diameter of the rod and its insulation was 7.2 mm at
the place of observation. The rod appears as the central shadow in Fig. 4.

We find that a cylindrical luminous surface, probably coincidental with a
shock wave, expands from the surface of the rod. Its expansion velocity
decreases from an initial value of 1.1 mm/μsec. After 5 μsec this wave,
having moved 5 mm from the surface of the rod, has attenuated into a sound
wave having a speed of 0.4 mm/μsec.

The radiation from the hot plasma reached a maximum in 2 μsec; this
maximum coincides with the current maximum of 22 kA recorded by the Rogowski
coil. At the time of greatest luminosity and largest current flow, the
luminous plasma has reached a thickness of 2.4 mm. At this time the diameter
of the radiating plasma surface is 12 mm. The maximum current density in the
plasma sheath is, therefore, found to be 30.4 kA/cm^2, and the total radiating
area A_{rad} of the luminous front surrounding the rod is 301 cm^2.

In addition, examination of the streak photographs offers an explanation
for the slow rise time of the current pulse of Fig. 3. The plasma sheath acts
as a time-dependent resistor that determines the current rise time. Initially
the current is restricted to a very thin sheath of low conductance. Baranov
et al.[6] also observed the appearance of streamers in the initial phases of a
sliding discharge which may be responsible for the low conductance, although
we have not observed any such streamers within the time and spatial resolution
of our equipment and experimental conditions. We believe that in our exper-
iments the resistivity of the discharge is limited by the slow gasdynamic
expansion of the conducting sheath. As the sheath expands gasdynamically, the
plasma cross section and its conductivity increase rapidly and simultaneously.
After about 2 to 3 μsec, the energy stored in the capacitor has essentially
been dissipated and the plasma expansion slows down.

We find, in agreement with the streak camera records, that the duration
of the light pulse produced by the plasma is considerably shorter than the
current pulse. Figure 5 shows the light pulse as seen by the photomultiplier

11
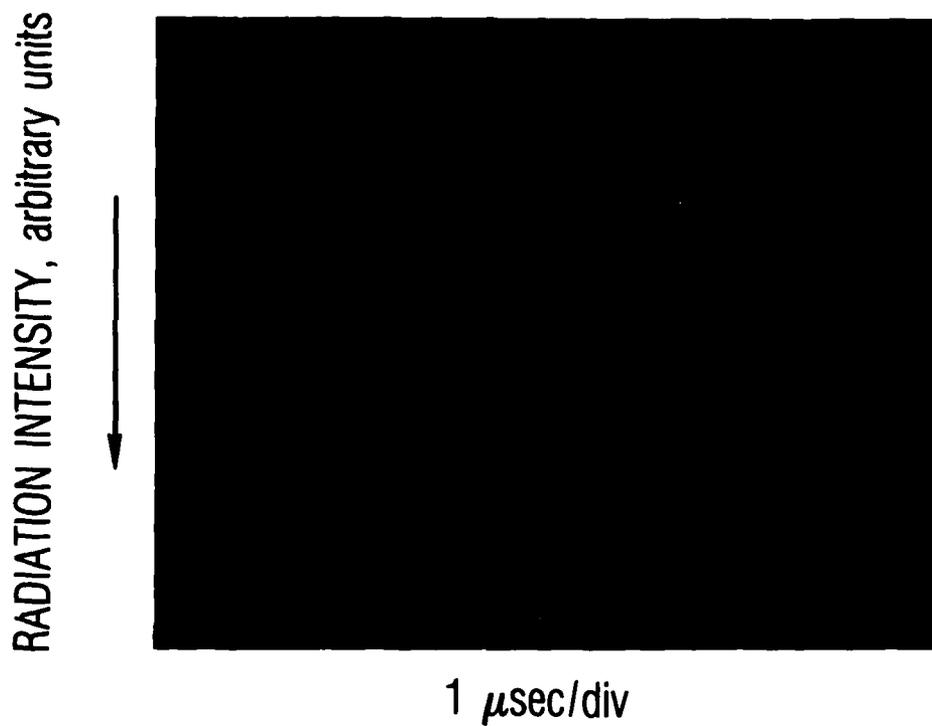
Fig. 5. Oscilloscope Record of Emitted Radiation at 350 to 450 nm in 300 Torr Argon at 50 kV (1/4-in. Rod) (Kapton Insulation)

through a 350 to 450-nm Corning filter. The response time of the photomulti-
plier circuit was of the order of 0.1 μsec. From a series of measurements we
inferred that the FWHM duration of the light pulse varies between 1.1 and
1.8 μsec for constant conditions of 50 kV and 300 Torr of argon. The observed
shortening of the light output compared to the current pulse duration is
probably caused by the optical and physical thinness of the plasma sheath.

Initially the plasma is highly transparent and its emissivity is low. As
the electron density and the physical thickness of the sheath increase
together, the emissivity of the plasma rapidly reaches a maximum that results
in the observed emission peak. The duration of the optical pulse is also
found to be influenced by the insulation material. When the Kapton insulation
was covered with a second wrapping of Teflon tape, we observed a further
shortenening of the radiation pulse to 0.8 μsec, as shown in Fig. 6. We
attribute this effect to the quenching of the discharge by fluorine compounds
evaporated from the surface of the tape. Unfortunately, this strong quenching
also results in a loss of emitted radiation energy. For this reason and
because of the short lifetime of the Teflon wrapping, these experiments were
abandoned.

Table 1 presents the radiation energies measured with the calorimeter.
All measurements were obtained at a charging voltage of 50 kV and a pressure
of 300 Torr of argon. The time-integrated, total energy fluence radiated by
the entire plasma surface surrounding the rod is given as measured by a number
of different cut-off filters. Division by the FWHM duration of the radiation
pulse yields the emitted flux or power density. We measured a total energy of
146 J emitted into the wavelength region between 120 and 5000 nm; this corre-
sponds to 6.3% of the stored capacitor energy. Half of this energy, or
76.7 J, appeared in the VUV region between 140 and 210 nm. Taking into
account the pulse duration of 1.3 μsec and the total plasma surface area of
301 cm^2, this corresponds to a power flux of 196 kW/cm^2.

In a second series of experiments using a 1/2-in. rod, we found that the
electrical parameters differed by less than 10% from those of the 1/4-in. rod
under the same conditions of 300 Torr of argon and a total discharged energy
of 2.34 kJ at 50 kV.

RADIATION INTENSITY, arbitrary units
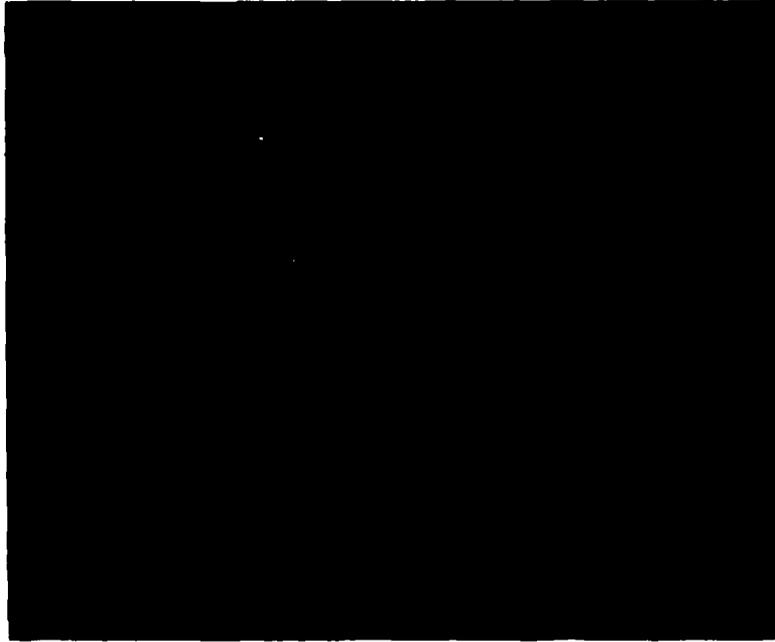
1 μsec/div

Fig. 6. Oscilloscope Record of Emitted Radiation (Same Conditions as in Fig. 5, but with Teflon Insulation)

Table 1. Spectral Energies Emitted from Sliding Discharge.
All measurements: argon at 300 Torr, charging
voltage = 50 kV, discharged energy = 2.32 kJ.

Filter	Wavelength Range, nm	1/4-in. Rod[a]		1/2-in. Rod[b]	
		Fluence, J/cm^2	Flux, kW/cm^2	Fluence, J/cm^2	Flux, kW/cm^2
Pyrex	320–1500	0.083	69	0.072	60
Quartz	235–3000	0.152	127	0.147	123
Suprasil	160–3000	0.357	298	0.160	134
MgF$_2$	120–5000	0.493	411	0.164	137

[a]For 1/4-in. rod: arc length = 75 cm, pulse duration = 1.3 µsec, plasma diameter = 1.21 cm, radiating area = 301 cm^2

[b]For 1/2-in. rod: arc length = 84 cm, pulse duration = 1.2 µsec, plasma diameter = 1.86 cm, radiating area = 491 cm^2

Streak camera pictures showed that the luminous front expanded initially at a slightly lower velocity of 1.0 mm/μsec, but reached full attenuation after 3 μsec. The maximum current under critically damped conditions was, as before, 22 kA. The plasma sheet at the time of maximum emission had an outer diameter of 1.86 cm and a thickness of 2.5 mm; this leads to a current density of only 17 kA/cm^2. In addition, the radiating surface of the 1/2-in. rod had an area of 491 cm^2 and was, therefore, 63% larger than that of the 1/4-in. rod.

As a consequence of the lower current density and the enlarged radiating surface, the spectral energy and intensity emitted from the 1/2-in. rod was found, as can be seen from Table 1, to be drastically lower than that of the 1/4-in. rod. The total, time-integrated energy emitted between 120 and 5000 nm was measured to be 81 J, which corresponds to only 3.5% of the stored electrical energy. The total power flux was 126 kW/cm^2. About half of the energy emitted from the 1/2-in. rod appeared in the visible region at wavelengths larger than 350 nm.

By subtracting the energies measured with the various filters from each other, one finds wavelength-averaged and time-integrated specific fluences and spectral intensities that are emitted in the various wavelength regions; these fluences and intensities are listed in Table 2. In our subtractions we ignored as negligible the contributions to the measured energies from the infrared region between 1500 and 5000 nm. From these data it is possible to calculate brightness temperatures T_B for the various spectral regions, where T_B is the temperature of the blackbody that radiates the measured intensity into the wavelength interval in question. Values for T_B thus obtained are also given in Table 2. Figure 7 shows the variation of the spectral intensity and Fig. 8 the brightness temperature for the two rods as a function of wavelength between 120 and 350 nm.

It is seen that the radiation emitted by the discharges cannot be described by a single blackbody temperature. The plasma of the 1/4-in. rod is, therefore, in a state of radiation nonequilibrium, emitting 2.8 kW/cm^2 nm in the VUV between 120 and 200 nm and only 58 W/cm^2 nm in the visible above

16

Table 2. Specific, Time-Integrated Fluence and Intensity as
a Function of Wavelength for the Two Discharges

Wavelength Center, nm	Width, nm	Specific Fluence, J/cm^2 nm	Specific Intensity, W/cm^2 nm	Brightness, Temperature, K
1/4-in. Rod:				
140	40	3.41E-3	2840.	17500
178	115	2.96E-3	2470.	17800
198	75	2.73E-3	2270.	17000
220	200	2.05E-3	1710.	17400
240	160	1.72E-3	1430.	16600
278	85	0.82E-3	680.	13550
910	1180	0.07E-3	60.	12280
1/2-in. Rod:				
140	40	1.02E-4	85.	11400
178	115	1.54E-4	129.	11100
198	75	1.52E-4	152.	10900
220	200	4.64E-4	386.	12600
240	160	5.54E-4	464.	13300
278	85	8.82E-4	735.	14900
910	1180	0.61E-4	51.	12050
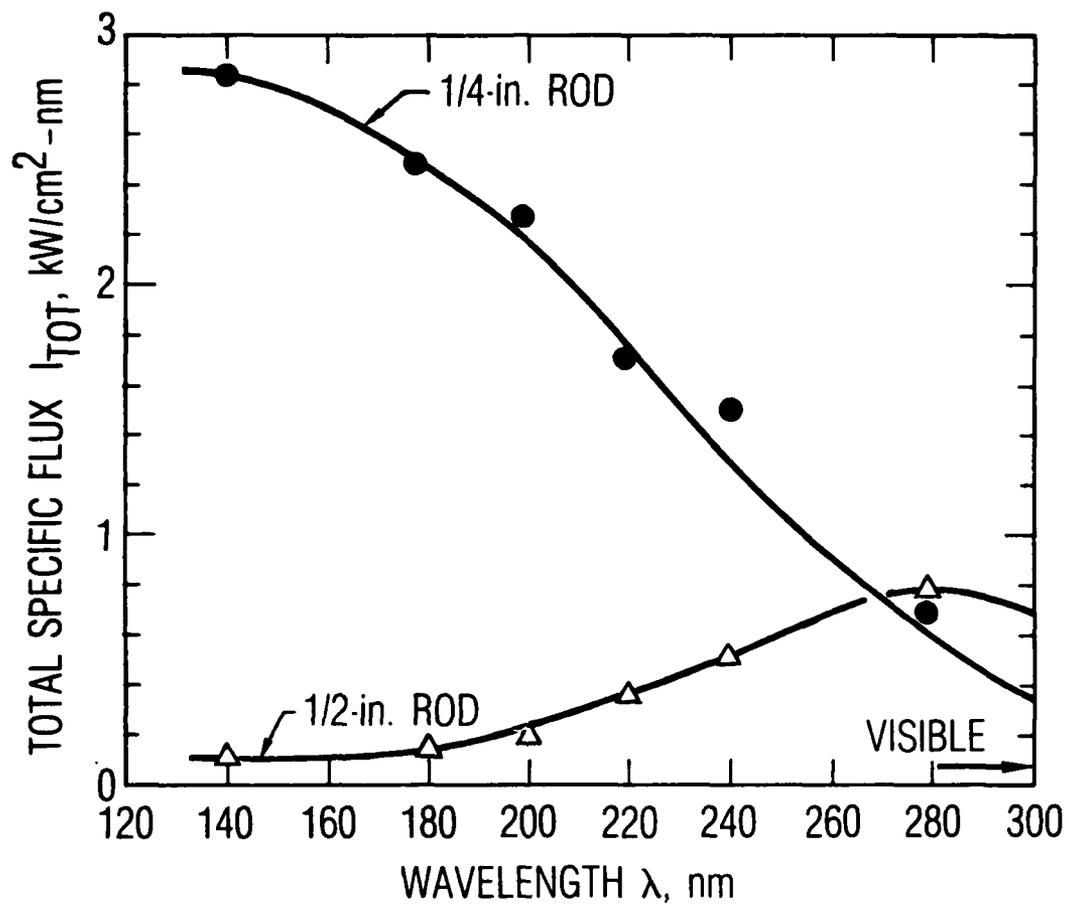
Fig. 7. Measured Spectral Intensity Distribution in 300 Torr Argon
at 50 kV

18
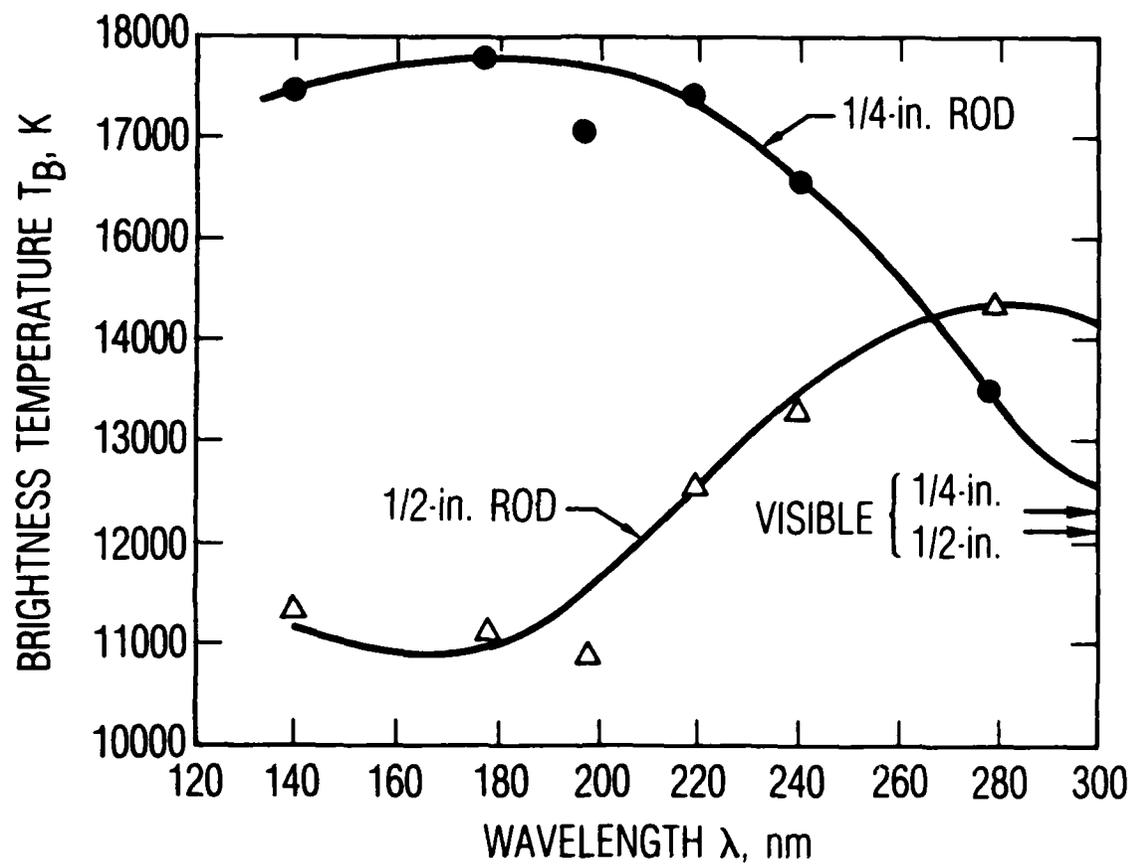
Fig. 8. Measured Brightness Temperature of Sliding Discharge in 300 Torr Argon at 50 kV

19

350 nm. The corresponding brightness temperatures are 17800 K in the VUV and 12300 K in the visible. Table 2 and Fig. 7 show that the maximum of the spectral intensity of the 1/2-in. rod has shifted to 280 nm, where the plasma emits a spectral flux of 0.7 kW/cm^2 nm; the brightness temperature of the 1/2-in. rod (see Fig. 8) reaches a maximum of 14900 K at this wavelength. In addition, the maximum flux and the brightness temperature are markedly lower than the corresponding values observed for the 1/4-in. rod.

In a few experiments we operated the discharge in an atmosphere of 300 Torr of xenon. The electrical characteristics of the discharge did not change markedly compared to those for argon, except for a lengthening of the current and radiation pulses, which is probably a consequence of the lower shock speed in the heavier xenon. The total energy emitted into the 120 to 5000 nm region for the 1/4-in. rod was found to be only 100 J at 50 kV, about 30% of which appeared in the visible above 350 nm. These experiments show that, in contrast to the case for regular flashlamps, a xenon atmosphere offers no advantages over argon.

IV. CONCLUSIONS

We have found that the optically thin plasma sheath, formed by a discharge that slides coaxially along a metallic rod covered with a thin insulating film of Kapton, is an excellent source of intense UV radiation. The emitted radiation has a wavelength dependence that is highly non-Planckian. Increasing the current density in the plasma sheath, by decreasing the diameter of the rod at a fixed electric energy input, allows one to shift the emission maximum from the visible into the vacuum ultraviolet region of the spectrum.

We have also investigated the electrical characteristics of such a discharge, and find that critical damping can be achieved by the proper choice of the pressure and the gas in which the discharge operates. The current-pulse duration is determined by the velocity of the gasdynamic expansion of the plasma sheath away from the surface of the insulated rod. The duration of the radiation pulse can also be affected by material evaporated from the insulation covering the rod.

In particular we studied the plasma sheath produced by a sliding discharge surrounding a 6.1-mm aluminum rod covered by a Kapton film 0.05 to 1.02 mm thick in an argon atmosphere at 300 Torr. An energy of 2.32 kJ, stored in a fast capacitor of 1.85 μF charged to 50 kJ, was discharged. The discharge circuit was found to have an inductance of 225 nH. The maximum current density in the plasma sheath was 30.4 kA/cm^2, and the FWHM duration of the critically damped current pulse was found to be 2.2 μsec.

The plasma emitted radiation having a maximum intensity of 2.8 kW/cm^2 nm at 140 nm. This corresponds to a brightness temperature of 17800 K. In the visible spectrum the intensity was found to be only 58 W/cm^2 nm, which corresponds to a brightness temperature of 12280 K.

Integrated over the wavelength region from 140 to 210 nm and over the surface area of the plasma sheath, the discharge emitted 76.7 J, or 3.3% of the stored electrical energy, in radiation in the vacuum UV in a pulse of 1.3 μsec FWHM duration.

21

REFERENCES

1.   For a sampling of the recent literature see the following:

D. Yu. Zaroslov, G. P. Kuzmin, and V. F. Tarasenko, "Sliding Discharges in CO_2 and Excimer Lasers," Radio Engineering and Electrophysics 29, 1 (1984).

V. Yu. Baranov, V. M. Borisov, Yu. B. Kiryukhin, S. G. Mamonov, Yu. Yu. Stepanov, and O. B. Kristoforov, "UV-Preionized Rare Gas Halide Lasers with Plasma Electrodes," Proceedings of the International Conference on Lasers 1981 (Orlando, Fla., 14-18 December 1981).

V. Yu. Baranov, V. M. Borisov, A. M. Davidivskij, and O. B. Kristoforov, "The Use of a Discharge on a Dielectric Surface for Preionization of Excimer Lasers," Sov. J. Quant. Electron. 11, 42 (1980).

A. K. Zhigalkin and Yu. L. Sidorov, "Extended Preionization UV Source for Pulsed Lasers," Instrum. and Exp. Tech. 6, 1473 (1980).

S. F. Zhuravlev, V. G. Karelskij, Yu. I. Kozlov, V. K. Orlov, A. K. Piskunov, Yu. V. Romanenko, and Yu. I. Shcherbakov, "Electric-Discharge Chemical HF Laser Operating at High-Pulse Repetition Frequency," Sov. J. Quant. Electron 11, 546 (1980).

D. Yu. Zaroslav, N. V. Karlov, and G. P. Kuzmin, "Use of a Surface Discharge for Preionization of Gases in a Discharge Laser," Sov. J. Quant. Electron. 8, 1048 (1978).

2.   R. E. Beverly III, "Applications of Surface Discharges for UV Photodissociation, Photoinitiation, and Preionization of Gas-Flow Lasers," Proceedings of the 5th International Conference on Gas Flow and Chemical Lasers (Oxford, 20-24 August 1984).

A. S. Gasheev, A. Z. Zaretskii, G. A. Kirillov, S. B. Kormer, Yu. P. Kuzmichev, Yu. V. Kuratov, A. I. Kucherov, V. M. Murugov, N. A. Nitochkin, N. N. Rukavishnikov, A. V. Ryadov, V. A. Samylin, S. A. Sukharev, and V. I. Shemyakin, Sov. Tech. Phys. Lett. 7, 585 (1981).

A. V. Beloserkovets, V. A. Gajdash, G. A. Kirillov, S. B. Kormer, V. A. Krotov, Yu. V. Kuratov, S. G. Lapin, V. M. Murugov, N. N. Rukavishnikov, V. A. Samylin, N. A. Cherkesov, and V. I. Shemyakin, "An Iodine Nanosecond-Pulse Amplifier," Sov. Tech. Phys. Lett. 5, 80 (1978).

O. B. Danilov, A. P. Zhevlakov, S. A. Tulskij, and I. L. Yachev, "Investigation of a High-Efficiency Photodissociation Laser Operating in the Free-Lasing Regime," Sov. J. Quant. Electron. 12, 786 (1981). A. S. Bashkin, P. G. Grigoriev, A. N. Oraevskii, and A. B. Skvortsov, "High-Power, 1-μsec Ultraviolet Radiation Source for Pumping of Gas Lasers," Sov. J. Quantum Electron. 6, 994 (1976).

S. I. Andreev, M. P. Vanyukov, and E. V. Daniel, Sov. Phys. Tech. Phys. 12, 1110 (1966).

3.   D. Yu. Zaroslov, G. P. Kuzmin, and V. P. Tarasenko, "Sliding Discharge in CO_2 and Excimer Lasers," Radio Engineering and Electrophysics 29, 1 (1984).

Yu. S. Protasov, Paper presented at the International Conference on Lasers 1984 (San Francisco, 22-28 November 1984).

A. S. Kamrukov, N. P. Kozlov, and Yu. S. Protasov, "The Radiation Spectrum of a Plasma Focus in the Quantum Energy Range from 0.64 to 350 eV," Sov. Phys. Dokl. 22, 740 (1978).

4.   D. Yu. Zaroslov, G. P. Kuzmin, and V. P. Tarasenko, "Sliding Discharge in CO_2 and Excimer Lasers," Radio Engineering and Electrophysics 29, 1 (1984).

5.   S. I. Andreev, E. A. Zobov, A. N. Sidorov, and V. D. Kostousov, "An Investigation of a Long Sliding Spark," Sov. App. Mech. and Tech. Phys. 1, 103 (1980).

6.   Yu. V. Baranov, V. M. Borisov, F. I. Vysikaylo, Yu. B. Kiriyukhin, and O. B. Kristoforov, "Investigation of the Formation and Evolution of a Sliding Discharge," Preprint No. 3473/7, Kurchatov Institute of Atomic Energy (Moscow, 1981).

LABORATORY OPERATIONS

The Aerospace Corporation functions as an "architect-engineer" for national security projects, specializing in advanced military space systems. Providing research support, the corporation's Laboratory Operations conducts experimental and theoretical investigations that focus on the application of scientific and technical advances to such systems. Vital to the success of these investigations is the technical staff's wide-ranging expertise and its ability to stay current with new developments. This expertise is enhanced by a research program aimed at dealing with the many problems associated with rapidly evolving space systems. Contributing their capabilities to the research effort are these individual laboratories:

Aerophysics Laboratory: Launch vehicle and reentry fluid mechanics, heat transfer and flight dynamics; chemical and electric propulsion, propellant chemistry, chemical dynamics, environmental chemistry, trace detection; spacecraft structural mechanics, contamination, thermal and structural control; high temperature thermomechanics, gas kinetics and radiation; cw and pulsed chemical and excimer laser development including chemical kinetics, spectroscopy, optical resonators, beam control, atmospheric propagation, laser effects and countermeasures.

Chemistry and Physics Laboratory: Atmospheric chemical reactions, atmospheric optics, light scattering, state-specific chemical reactions and radiative signatures of missile plumes, sensor out-of-field-of-view rejection, applied laser spectroscopy, laser chemistry, laser optoelectronics, solar cell physics, battery electrochemistry, space vacuum and radiation effects on materials, lubrication and surface phenomena, thermionic emission, photo-sensitive materials and detectors, atomic frequency standards, and environmental chemistry.

Computer Science Laboratory: Program verification, program translation, performance-sensitive system design, distributed architectures for spaceborne computers, fault-tolerant computer systems, artificial intelligence, micro-electronics applications, communication protocols, and computer security.

Electronics Research Laboratory: Microelectronics, solid-state device physics, compound semiconductors, radiation hardening; electro-optics, quantum electronics, solid-state lasers, optical propagation and communications; microwave semiconductor devices, microwave/millimeter wave measurements, diagnostics and radiometry, microwave/millimeter wave thermionic devices; atomic time and frequency standards; antennas, rf systems, electromagnetic propagation phenomena, space communication systems.

Materials Sciences Laboratory: Development of new materials: metals, alloys, ceramics, polymers and their composites, and new forms of carbon; non-destructive evaluation, component failure analysis and reliability; fracture mechanics and stress corrosion; analysis and evaluation of materials at cryogenic and elevated temperatures as well as in space and enemy-induced environments.

Space Sciences Laboratory: Magnetospheric, auroral and cosmic ray physics, wave-particle interactions, magnetospheric plasma waves; atmospheric and ionospheric physics, density and composition of the upper atmosphere, remote sensing using atmospheric radiation; solar physics, infrared astronomy, infrared signature analysis; effects of solar activity, magnetic storms and nuclear explosions on the earth's atmosphere, ionosphere and magnetosphere; effects of electromagnetic and particulate radiations on space systems; space instrumentation.

END

DTIC

9 — 86